



## Cyclic Voltammetry Study of Ice Formation in the PEFC Catalyst Layer during Cold Start

Shanhai Ge\* and Chao-Yang Wang\*<sup>z</sup>

Electrochemical Engine Center, and Department of Mechanical and Nuclear Engineering, The Pennsylvania State University, University Park, Pennsylvania 16802, USA

A cyclic voltammetry technique has been developed to investigate the effect of ice formation in the cathode catalyst layer (CL) on electrochemically active Pt area during and post-subzero startup of a polymer electrolyte fuel cell (PEFC). It was found that the Pt area decreases after each cold start and the Pt area loss increases with the product water generated during cold start. We hypothesize that the Pt area loss is caused by ice precipitated between Pt particles and ionomers during cold start. After startup from a subzero temperature and warmup to 25°C with all ice in the CL melted, the cell remains subject to Pt area loss, but this loss at 25°C is substantially reduced. We also find that subsequent cell operation at 70°C and 1 A/cm<sup>2</sup> for 2 h is very effective for recovering the active Pt area and cell performance. Both permanent loss in the active Pt area and cell performance degradation due to structural alteration of the cathode CL by the presence of ice increase gradually with the cold-start cycle number and become more severe for cold start from -30°C than from -10 and -20°C. In addition, startup from a subzero temperature appears to have no influence on the electrochemically active Pt area of the anode CL. It is suggested that the ice amount present in the CL holds a key to determine the temporary Pt area loss due to ice formation as well as permanent performance degradation resulting from cold-start cycling.

© 2007 The Electrochemical Society. [DOI: 10.1149/1.2784166] All rights reserved.

Manuscript submitted June 20, 2007; revised manuscript received August 8, 2007. Available electronically October 29, 2007.

Polymer electrolyte fuel cells (PEFCs) promise clean, energy-efficient power for future automobiles. However, there remain many challenges for commercialization, among which are survivability and startup capability in a subzero environment. Product water becomes ice or frost upon startup when the PEFC internal temperature is below the freezing point of water. The product ice may reduce the three-phase interface for electrochemical reaction and the open pore volume for oxygen diffusion in the cathode catalyst layer (CL). The presence of ice may also result in damage to the structures and materials of a membrane-electrode assembly (MEA).

Few studies in the literature have touched upon PEFC cold start and associated MEA durability.<sup>1-15</sup> Oszipok et al.<sup>1,2</sup> demonstrated that ice formation results in performance degradation and a decrease in the electrochemically active area (ECA) of the cathode CL measured at room temperature prior to and subsequent to subzero startup. Kagami et al.<sup>3</sup> showed that a cell can operate at a subfreezing temperature by balancing the amount of product water with water removed from the cell through exhaust gases. However, the simulation results of Hishinuma et al.<sup>4</sup> indicated that startup is difficult from temperatures below -5°C because a large quantity of gas to remove product water would simultaneously carry away the heat generated by the cell.

McDonald et al.<sup>5</sup> observed that the proton conductivity of Nafion 112 membrane does not change and no degradation in catalyst performance occurs for the dry MEA subjected to freeze/thaw cycling between -40 and 80°C. Wilson et al.<sup>6</sup> showed that freezing at -10°C is not detrimental to the MEA integrity despite its high water content. Cho et al.<sup>7</sup> reported that the performance of a cell containing membrane with high water content is degraded after freeze/thaw cycling between -10 and 80°C. However, if the cell is purged with dry gas for 20 min, almost no performance degradation or increase in membrane resistance can be observed after the freeze/thaw cycling.<sup>8</sup> Guo and Qi<sup>9</sup> showed that freeze/thaw cycles caused the catalyst layer (CL) of a fully hydrated MEA to crack, but freeze/thaw cycles did not lead to apparent damage of CL if the cell was purged with dry gases for 1 min. St-Pierre et al.<sup>10</sup> showed that cool purge (purge with dry gas at 20°C) is better than hot purge (purge with dry gas at 85°C). Performance losses were not observed in a cell purged with dry gas at 20°C after the freeze/thaw cycling. While there is much controversy in the literature on MEA durability from freeze/thaw cycles and its dependence on the membrane water

content, the current consensus is that MEA can survive many hundreds of freeze/thaw cycles between a subzero temperature, such as -40°C, and an operating temperature, such as 80°C. Note, however, that freeze/thaw thermal cycling does not involve net water production in the CL, while subzero startup does. The latter is the subject of the present study. Mao et al.<sup>11</sup> were among the first to study MEA degradation mechanisms resulting from cold start (i.e., with water production).

To elucidate the fundamental principles underlying cold start of an automotive PEFC from -20°C and lower, a series of experimental and modeling studies were reported by Wang's group.<sup>16-21</sup> Ge and Wang<sup>16</sup> used a transparent cell and silver mesh as gas diffusion layer (GDL) to visualize ice formation on the catalyst layer in an operating fuel cell, and showed that the freezing-point depression of water in the CL pores is no larger than 2°C. Later, using a realistic carbon paper GDL punched with microholes, Ge and Wang<sup>17</sup> further refined the measurement of the freezing-point depression of water in the cathode CL to be 1.0 ± 0.5°C. Therefore, for a practical fuel cell vehicle cold start that is typically from -20°C or lower, the freezing-point depression is inconsequential. Mao and Wang<sup>18</sup> delineated the governing physics of coupled water and heat balance in PEFC cold start and presented an analytical model to forecast key parameters such as the initial membrane water content prior to cold start and thermal mass of bipolar plates. Mao et al.<sup>19</sup> further developed a multiphase, transient three-dimensional (3D) model to simulate cold-start performance. The model accounted for ice/frost precipitation and growth in the cathode CL and GDL, water transport at very low temperatures, heat transfer with phase transition, oxygen transport, electrochemical kinetics, and their mutual interactions. The 3D numerical model was extensively validated against the experimental data of Tajiri et al.<sup>20,21</sup> with good agreement. In addition, Tajiri et al.<sup>20,21</sup> described experimental protocols and presented extensive test data aimed to establish the fundamentals of PEFC cold start.

Obviously, understanding ice formation in the cathode CL is a key to self-startup and longevity of a PEFC. During cold start from very low temperatures, water generated in CL, after absorption by and transport into the membrane, precipitates as solid ice (with ice density ~0.92 g/cm<sup>3</sup>). The presence of ice in the cathode CL imposes two effects: one is volumetric blockage to reduce oxygen diffusion through the CL, and the other is surface coverage to reduce the ECA. Cho et al.<sup>7</sup> used cyclic voltammetry (CV) to study the effect of thermal cycles from 80 to -10°C on the ECA and Oszipok et al.<sup>1</sup> used it to study degradation of the porous CL structure after cold start. In both studies of Cho et al. and Oszipok et al., CV

\* Electrochemical Society Active Member.

<sup>z</sup> E-mail: cxw31@psu.edu

tests were carried out after cold start at room temperature and there was no ice present in the CL. As such, their ECA results reflect CL damage after a completed ice formation and melting cycle.

In this work, we carry out CV experiments during cold start to investigate the effect of ice formation on H-desorption at the Pt surface. The active Pt areas during cold start from  $-10^{\circ}\text{C}$ ,  $-20^{\circ}\text{C}$  and  $-30^{\circ}\text{C}$  are measured and correlated with the amount of product water. In addition, the active Pt area after the cell warms up to  $25^{\circ}\text{C}$  is also measured to understand the influences of cold start on cell performance post-cold start.

### Experimental

A catalyst coated membrane based on an 18  $\mu\text{m}$  thick Gore-Select membrane was sandwiched between two polytetrafluoroethylene-proofed carbon papers with microporous layer (GDL 20BB, SGL) as the anode and cathode gas diffusion layers, respectively. The flow field plates for testing the MEA were made of graphite and were clamped between stainless steel plates. One-pass serpentine flow channels with a cross section of  $0.8 \times 0.8$  mm were machined onto the surface of graphite plates. The width of the land is 0.8 mm. The Pt loadings in the anode and cathode catalyst layers are both  $0.4$   $\text{mg}/\text{cm}^2$ . The active area of the electrode is  $5$   $\text{cm}^2$ .

The cell was connected to a fully computer-controlled fuel cell test station (Teledyne). The cell was preconditioned by operating it with fully humidified hydrogen and air at low stoichiometric ratios ( $\xi$ ) at  $80^{\circ}\text{C}$  for 6 h. An environmental chamber was used to control cell temperature during cold start and CV tests at subzero temperatures ( $-10$ ,  $-20$  or  $-30^{\circ}\text{C}$ ). The experiment procedure is detailed as follows:

1. A polarization curve before each cold start experiment was obtained at  $70^{\circ}\text{C}$  as a base line of the cell performance. For the current-voltage curve measurement, the cell was operated in the constant-current mode and the cell potential was averaged over 2 min. The pressures of the anode and cathode were both kept at 1 atm (absolute). The relative humidity of the inlet hydrogen and air was both kept at 100%. Flow rates of the hydrogen and air were kept at 100 and 400 mL/min under standard temperature and pressure (STP), respectively.

2. The cell was then cooled down to  $25^{\circ}\text{C}$ , and cyclic voltammograms (CVs) were taken at this temperature. This CV serves as a reference prior to cooldown and cold start.

3. The cell temperature increased back to  $55^{\circ}\text{C}$ , and the cell was operated with fully humidified hydrogen and air for 30 min. Then both sides of the cell were purged with dry nitrogen at the same time at  $55^{\circ}\text{C}$  for 2 min. The flow rates of the anode and cathode purging gases were 400 and 900 mL/min (STP), respectively.

4. After gas purge, the cell was cooled down to a prescribed startup temperature ( $-10^{\circ}\text{C}$ ,  $-20^{\circ}\text{C}$  or  $-30^{\circ}\text{C}$ ) and a CV test was carried out at this subzero temperature immediately prior to cold start. This CV characterizes the CL state after cooldown but before cold start.

5. Dry hydrogen and air were then fed to the cell and the flow rates of hydrogen and air were 25 and 50 mL/min (STP,  $\xi_{\text{H}_2} = 14.35$  and  $\xi_{\text{air}} = 12.06$ ), respectively. The cell was discharged at the current density of  $50$   $\text{mA}/\text{cm}^2$  during cold start and the discharge was interrupted when a prescribed product water (e.g., 0.1, 0.2, 0.3, etc.  $\text{mg}/\text{cm}^2$ ) was achieved or cell potential dropped to 0.1 V. Immediately after this, dry nitrogen was fed to the cathode and CV was performed. This CV characterizes the CL state in the presence of product ice.

6. The cell was then warmed up to  $25^{\circ}\text{C}$ , and a CV test was carried out again. This CV characterizes the state of CL post-cold start in which the ice in CL melted but liquid water could well remain inside micropores of the CL.

7. The cell was finally operated at  $70^{\circ}\text{C}$  for 2 h to recover cell performance and to obtain a polarization curve. The gas pressures, gas flow rates and relative humidity were the same as those at step 1.

8. Steps 1 through 7 were repeated for each prescribed amount of product water.

The scan speed for all CV tests was  $50$   $\text{mV}/\text{s}$ . When CV tests were carried out at  $25^{\circ}\text{C}$ , water-saturated nitrogen and hydrogen were used in the working and counter electrodes, respectively. The hydrogen electrode was also used as the reference electrode. The flow rates of nitrogen and hydrogen were both  $100$   $\text{mL}/\text{min}$ . When CV tests were carried out at a subzero temperature, dry nitrogen and hydrogen were fed to the working and counter electrodes (the reference electrode), respectively. The flow rates of nitrogen and hydrogen were both  $40$   $\text{mL}/\text{min}$  during CV test at a subzero temperature. The working electrode is always the cathode except for Fig. 14 where the working electrode is the anode.

### Results and Discussion

Before the cell was cooled down to a prescribed startup temperature, both sides of the cell were purged with dry nitrogen at the same time at  $55^{\circ}\text{C}$  for 2 min. This purge operation can remove water in the channel, GDL, MPL, CL and membrane, thus creating a favorable initial condition to accommodate water produced during cold start. Our previous studies showed that 2 min purge operation can reduce the water content of the membrane to approximately  $6.0$  mol  $\text{H}_2\text{O}/\text{mol SO}_3$ .<sup>16,17</sup>

Figure 1 compares the cyclic voltammograms at temperature of  $25^{\circ}\text{C}$  prior to and post-cold start. The startup temperature is  $-10^{\circ}\text{C}$ . Between the first and the sixth cold start experiments, the amount of water produced in cold start is 0.10, 0.30, 0.50, 0.70, 0.90, and  $0.98$   $\text{mg}/\text{cm}^2$ , respectively. In contrast, Fig. 2 shows the CVs at temperature of  $-10^{\circ}\text{C}$  prior to and post-cold start. The electrochemically active Pt surface area of the cathode CL is calculated as follows and listed in Table I

$$A_{\text{Pt}} = \frac{Q_D}{2.1W_{\text{Pt}}} \quad [1]$$

where  $W_{\text{Pt}}$  is the total Pt loading (g) in the electrode. In this work,  $W_{\text{Pt}}$  is equal to  $2 \times 10^{-3}$  g (i.e.,  $0.4$   $\text{mg}/\text{cm}^2$  for a  $5$   $\text{cm}^2$  electrode). The constant of  $2.1$   $\text{C}/\text{m}^2$  (or  $210$   $\mu\text{C}/\text{cm}^2$ ) in the denominator represents the H-desorption charge per  $\text{m}^2$  of a smooth Pt surface, assumed to be constant in the temperature range between  $-30^{\circ}\text{C}$  and  $25^{\circ}\text{C}$ .  $Q_D$  is the total Coulombic charge (C) integrated under the hydrogen desorption region from 0.05 to 0.45 V vs the hydrogen reference electrode (at low temperatures, such as  $-30^{\circ}\text{C}$ , this region is about 0.05–0.60 V), after correction for the double-layer capacitance of the carbon support and Pt catalyst. That is

$$Q_D = \int_{v_1}^{v_2} \frac{\Delta i dV}{\nu} \quad [2]$$

where  $\nu$  is the scan speed of CV (V/s).

Table I summarizes the measurement data of active Pt area prior to and post each cold start at temperatures of  $-10$  and  $25^{\circ}\text{C}$ . A Pt area loss ratio is defined as

$$R_{A,\text{loss}} = 1 - \frac{A_{\text{Pt,Post}}}{A_{\text{Pt,Prior}}} \quad [3]$$

Although the relative humidity and flow rate of gases for CV tests performed at  $25^{\circ}\text{C}$  (RH = 100%) and  $-10^{\circ}\text{C}$  (RH = 0%) are different, the RH conditions inside the cathode CL are believed to be sufficiently wet in both cases. Consequently, the active Pt surface area calculated from CV remains virtually the same (within measurement errors) between  $25^{\circ}\text{C}$  and  $-10^{\circ}\text{C}$  prior to cold start, as can be seen from Table I. For example, prior to the fifth cold start the active Pt areas from CV are  $77.56$  and  $77.88$   $\text{m}^2/\text{g}$  at  $25$  and  $-10^{\circ}\text{C}$ , respectively. In addition, there exists clear evidence of Pt area loss before and after each cold start and this loss increases with the product water involved in each cold start. At  $-10^{\circ}\text{C}$ , the Pt area loss is caused by the ice formation in CL during cold start. This Pt loss is

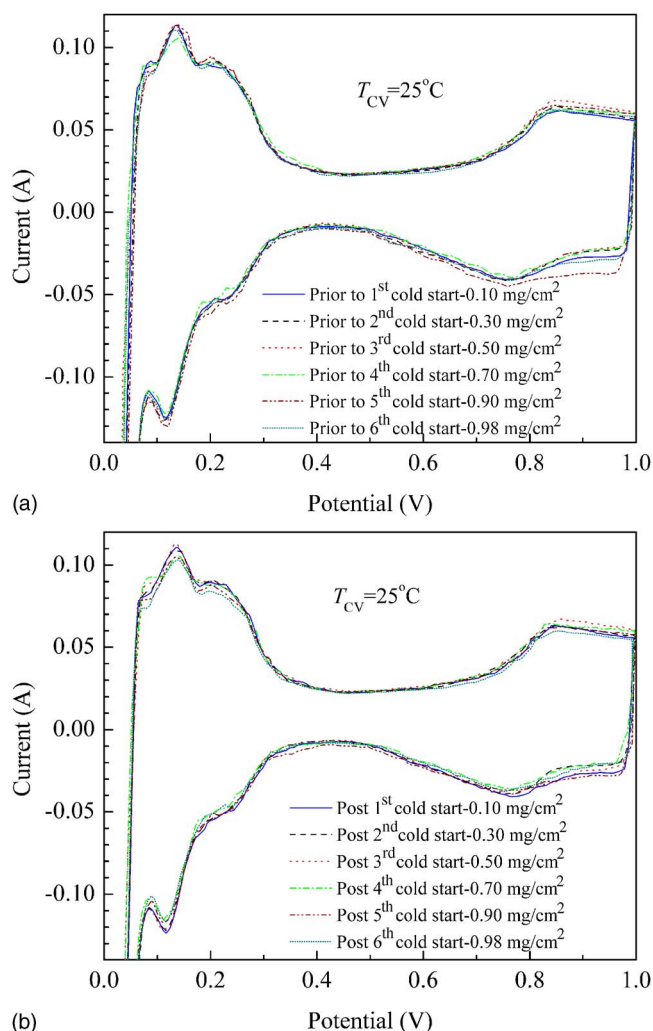


**Figure 1.** (Color online) Cyclic voltammograms (CVs) of the cathode at 25°C: (a) prior to cold start, and (b) post-cold start. (Cold start conditions:  $T_{\text{cell}} = -10^{\circ}\text{C}$ ,  $i = 0.05 \text{ A/cm}^2$ . CV conditions:  $T_{\text{CV}} = 25^{\circ}\text{C}$ ,  $\nu = 50 \text{ mV/s}$ ,  $F_{\text{N}_2} = F_{\text{H}_2} = 100 \text{ mL/min}$ ,  $\text{RH}_{\text{N}_2} = \text{RH}_{\text{H}_2} = 100\%$ .)

substantial and amounts to 38.9% with the product water of 0.98 mg/cm<sup>2</sup> generated in the cold start. After cold start at  $-10^{\circ}\text{C}$  and warm-up to  $25^{\circ}\text{C}$ , the cell is still subject to Pt area loss, but this loss at  $25^{\circ}\text{C}$  is substantially reduced and becomes 6.6% after the product water of 0.98 mg/cm<sup>2</sup>. The ice in the CL obviously melts; however, the nanostructure of the cathode CL is not resumed completely at this relatively low temperature ( $25^{\circ}\text{C}$ ) and hence part of the Pt surface area still passivates.

The reduction in Pt area due to ice formation can be explained by a hypothesis shown schematically in Fig. 3. As shown, ice precipitates in the CL in two forms: as ice sheets between Pt particles and ionomers and as ice/frost grown into open pores. The ice sheets between Pt particles and ionomers will lead to the Pt area loss, which can be measured by CV when ice sheets are still present at subzero temperatures. When the ice sheets melt and the cell temperature is raised to  $25^{\circ}\text{C}$ , Pt area loss diminishes but does not completely vanish because some liquid water resulting from ice melting may still be trapped between Pt particles and ionomers. Only when the CL is operated at elevated temperatures and large current density (or high heat generation), can liquid water trapped between Pt particles and ionomers be evaporated or diffused into ionomers, thus recovering the CL performance.

Experiments indeed confirm that the temporary loss in Pt area at  $25^{\circ}\text{C}$  post-cold start can be largely recovered by proper recovery

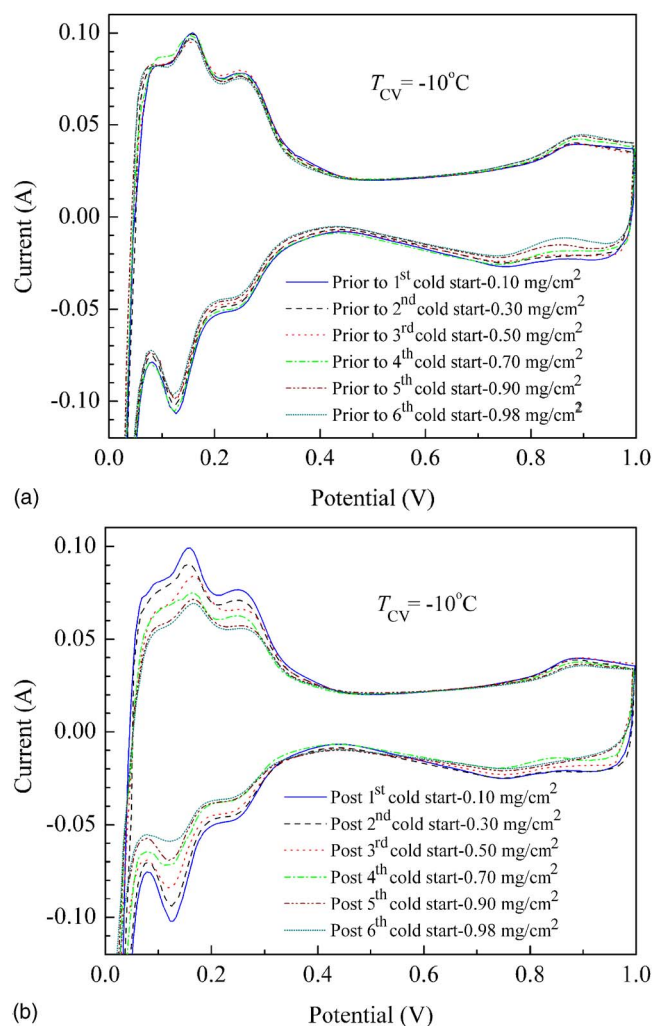


**Figure 2.** (Color online) CVs of the cathode at  $-10^{\circ}\text{C}$ : (a) prior to cold start, and (b) post-cold start. (Cold start conditions:  $T_{\text{cell}} = -10^{\circ}\text{C}$ ,  $i = 0.05 \text{ A/cm}^2$ . CV conditions:  $T_{\text{CV}} = -10^{\circ}\text{C}$ ,  $\nu = 50 \text{ mV/s}$ ,  $F_{\text{N}_2} = F_{\text{H}_2} = 40 \text{ mL/min}$ ,  $\text{RH}_{\text{N}_2} = \text{RH}_{\text{H}_2} = 0\%$ .)

operation. Figure 4 shows the voltage curves during two recovery operations at temperatures of 25 and  $70^{\circ}\text{C}$ . Figure 5 shows cell polarization curves before and after recovery operation. After the fifth cold start and after CV and cell polarization curve were taken at  $25^{\circ}\text{C}$ , water-saturated hydrogen and air were fed to the anode and cathode side of the cell. The current density was set to  $0.8 \text{ A/cm}^2$  and the cell voltage was recorded. After this 2 h operation at  $25^{\circ}\text{C}$ , the cell temperature increased to  $70^{\circ}\text{C}$  and water-saturated hydrogen and air were fed to the anode and cathode side of the cell. The current density was set to  $1 \text{ A/cm}^2$  and the cell voltage was recorded. It is found that operating the cell at  $25^{\circ}\text{C}$  is not effective to recover the cell performance, meaning that operating the cell with water saturated hydrogen and air at  $25^{\circ}\text{C}$  cannot resume the tight bonding of Pt particles with ionomers in the cathode CL. However, operating the cell at  $70^{\circ}\text{C}$  and  $1 \text{ A/cm}^2$  for 2 h is very effective to recover cell performance. The voltage increases rapidly in the first 8 min of operation. This “baking” process essentially raises the CL temperature sufficiently to promote evaporative removal of liquid water trapped inside the CL from cold start. After this “baking” procedure, the current density at  $25^{\circ}\text{C}$  and 0.5 V increases from 0.532 (before recovery operation) to  $0.824 \text{ A/cm}^2$  (after recovery operation), as shown in Fig. 5. In addition, the active Pt area can be mostly recovered from 72.92 to  $76.41 \text{ m}^2/\text{g}$  after the fifth cold start. However, there is also a permanent loss of  $1.15 \text{ m}^2/\text{g}$  ( $77.56\text{--}76.41$ )

Table I. Active Pt surface area measurements at 25, -10, -20 and -30°C

Cold start No.	Cold start temperature, $T_{\text{start}}$ (°C)	Amount of product water, $m_w$ (mg/cm <sup>2</sup> )	$A_{\text{Pt}}$ at 25°C prior to cold start (m <sup>2</sup> /g)	$A_{\text{Pt}}$ at 25°C post-cold start (m <sup>2</sup> /g)	$A_{\text{Pt}}$ at $T_{\text{start}}$ prior to cold start (m <sup>2</sup> /g)	$A_{\text{Pt}}$ at $T_{\text{start}}$ post-cold start (m <sup>2</sup> /g)
1	-10	0.100	78.54	78.44	78.72	77.59
2	-10	0.300	78.53	77.83	78.57	69.29
3	-10	0.500	78.10	76.71	78.29	61.14
4	-10	0.700	77.87	76.02	78.14	54.59
5	-10	0.900	77.56	72.92	77.88	48.48
6	-10	0.975	76.41	71.40	76.87	46.93
1	-20	0.100	78.16	76.25	78.46	76.31
2	-20	0.200	77.67	74.79	78.30	71.69
3	-20	0.300	76.79	73.14	77.41	64.16
4	-20	0.500	74.61	67.04	75.48	52.16
5	-20	0.700	73.88	65.53	74.31	44.38
6	-20	0.819	71.04	62.35	71.84	41.26
1	-30	0.100	78.32	76.11	78.83	75.39
2	-30	0.200	77.75	73.60	78.32	63.67
3	-30	0.300	76.33	68.40	76.62	52.64
4	-30	0.340	73.09	65.31	73.17	47.69

Pt area after the fifth cold start ( $m_w = 0.90$  mg/cm<sup>2</sup>;  $m_w$  = product water) at -10°C. The permanent loss of Pt area due to structural alteration of the cathode structure by the presence of ice increases gradually with the cold start cycle number.

The permanent degradation in cell performance during cold start cycle from -10°C is also evident from the polarization curves evaluated under normal conditions (70°C) after each cold start attempt. These curves are shown in Fig. 6 for the fresh MEA and after each cold start. It is shown that when the amount of product water during cold start is only 0.10 mg/cm<sup>2</sup>, almost no permanent degradation in cell performance is observed. When the product water is 0.90 mg/cm<sup>2</sup>, the permanent degradation in cell performance is up to 1.7% at 0.5 V (current density from 1.072 to 1.052 A/cm<sup>2</sup>).

Figure 7 shows cell voltage curves for startup from -10°C. For comparison, voltage curves for startup from -20 and -30°C are also shown in Fig. 7. Because ice generated in the cathode CL reduces the active Pt area as well as the rate of oxygen transport through the CL, the duration of cold start operation at -10°C is 208.8 s and the maximum amount of product water is 0.98 mg/cm<sup>2</sup>.

Figure 8 shows the CVs at temperature of -20°C prior to and post-cold start. Between the first to the sixth cold start, the amount of produced water is 0.10, 0.20, 0.30, 0.50, 0.70, and 0.82 mg/cm<sup>2</sup>, respectively. The duration of cold start operation at -20°C is

175.5 s and hence the maximum amount of product water is 0.82 mg/cm<sup>2</sup>, as shown in Fig. 7. Similar to the results of cold start from -10°C, the cell potential decreases in the first 2 s of start. Then due to increase of MEA hydration and membrane conductivity, the cell potential increases slightly. After 20 s into cold start, the cell potential drops due to ice formation in the CL. Table I lists the active Pt area prior to and post-cold start measured at different temperatures. Similar to the results of cold start at -10°C, within the statistical errors, the active Pt area calculated from CV remains almost the same at temperatures of 25°C and -20°C prior to cold start. However, it is evident from Table I that the active Pt area decreases after each cold start, and the loss increases with the product water. All the trends discussed earlier in relation to -10°C cold start are observed also for -20°C cold start, with the Pt area loss in all situations exacerbated. Figure 9 shows the polarization curves at 70°C during the cold start cycle from -20°C. The results further confirm that ice generated in the CL leads to permanent degradation

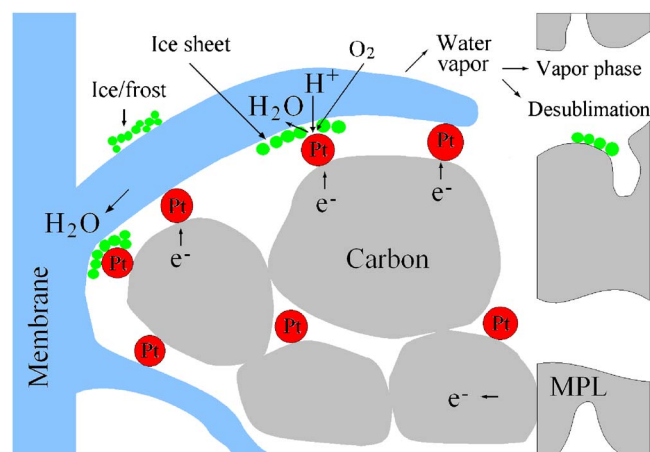


Figure 3. (Color online) Schematic of ice formation and microscale distribution in the cathode catalyst layer. Redrawn after Mao et al. (Ref. 19).

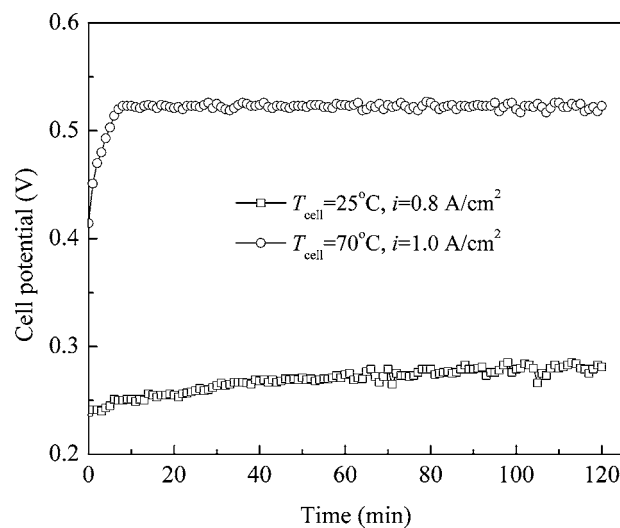
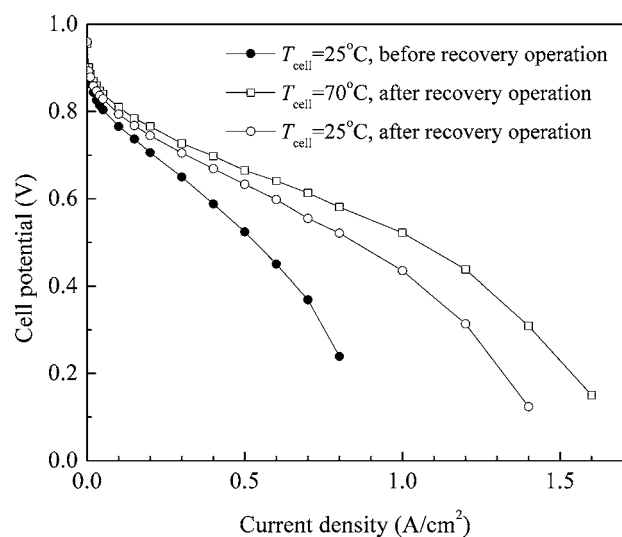


Figure 4. Cell voltage curves during performance recovery at different temperatures. ( $F_{\text{H}_2} = 100$  mL/min,  $F_{\text{air}} = 400$  mL/min,  $\text{RH}_{\text{H}_2} = \text{RH}_{\text{air}} = 100\%$ ,  $p_{\text{H}_2} = p_{\text{air}} = 1$  atm.)



**Figure 5.** Comparison of cell polarization curves before and after recovery operation. Recovery operation is to operate the cell at 70°C with water-saturated hydrogen and air at current density of 1.0 A/cm<sup>2</sup> for 2 h ( $F_{H_2} = 100$  mL/min,  $F_{air} = 400$  mL/min,  $RH_{H_2} = RH_{air} = 100\%$ ,  $p_{H_2} = p_{air} = 1$  atm.)

in cell performance. Comparing Fig. 9 with Fig. 6, it is apparent that the performance degradation resulting from cold start at  $-20^\circ\text{C}$  is more severe than that at  $-10^\circ\text{C}$ .

To fully understand the effects of product ice in the cathode CL on the electrochemically active Pt area and cell performance degradation, a series of experiments for cold start from  $-30^\circ\text{C}$  was also carried out. During the first to the fourth cold start, the amount of produced water is 0.10, 0.20, 0.30, and 0.34 mg/cm<sup>2</sup>, respectively. The duration of cold start from  $-30^\circ\text{C}$  is only 72.9 s and hence the maximum amount of product water is 0.34 mg/cm<sup>2</sup> at the current density of 50 mA/cm<sup>2</sup>, as shown in Fig. 7. Figure 10 shows the CVs at  $-30^\circ\text{C}$  prior to and post-cold start. Table I lists the active Pt area prior to and post-cold start measured at the temperatures of 25°C and  $-30^\circ\text{C}$ , respectively. The cell degradation is shown in Fig. 11,

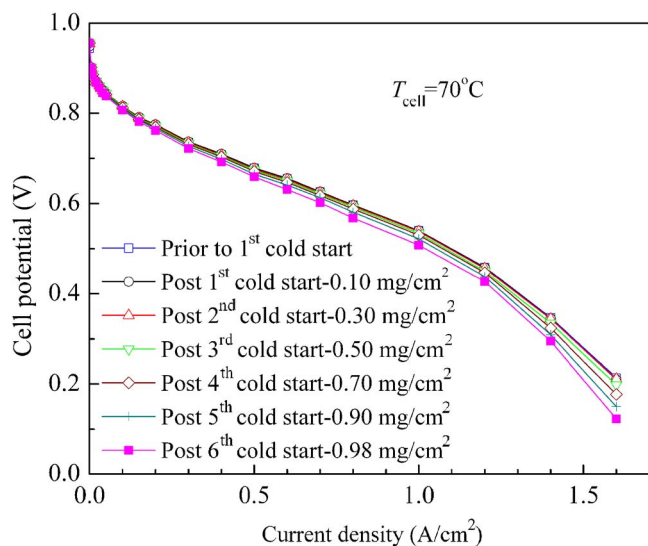


**Figure 6.** (Color online) Comparison of cell polarization curves in the cold start cycle from  $-10^\circ\text{C}$ . ( $T_{cell} = 70^\circ\text{C}$ ,  $F_{H_2} = 100$  mL/min,  $F_{air} = 400$  mL/min,  $RH_{H_2} = RH_{air} = 100\%$ ,  $p_{H_2} = p_{air} = 1$  atm; startup temperature:  $-10^\circ\text{C}$ .)

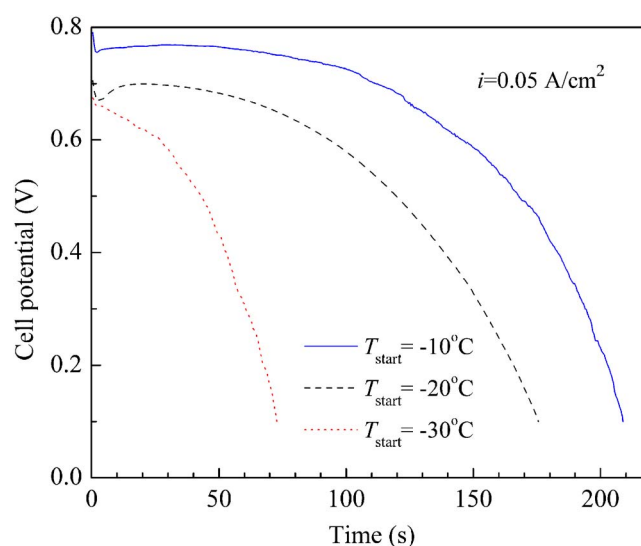


**Figure 7.** (Color online) Cell voltage curves for startup from different temperatures. (Purge conditions:  $T_{purge} = 55^\circ\text{C}$ ,  $t_{purge} = 120$  s. Startup conditions:  $i = 0.05$  A/cm<sup>2</sup>,  $F_{H_2} = 25$  mL/min,  $F_{air} = 50$  mL/min,  $RH_{H_2} = RH_{air} = 0\%$ ,  $p_{H_2} = p_{air} = 1$  atm.)

where it is seen that the degradation from the cold start cycle of  $-30^\circ\text{C}$  is most severe, and the Pt area loss at this startup temperature is also most severe.

Figure 12 summarizes all data of Pt area loss in the cathode CL after cold start at the cold start temperatures ( $-10$ ,  $-20$  and  $-30^\circ\text{C}$ ) and 25°C, respectively. The effect of product ice on Pt area loss is substantial and becomes more significant at lower temperatures, as can be seen from Fig. 12a. Up to 42.6% loss has been detected. This trend clearly indicates that ice formation in the cathode CL holds a key to understanding and controlling CL degradation resulting from cold start. After warmup to 25°C, the influence of product water created during cold start remains, but the Pt area loss diminishes to 10–12%, as shown in Fig. 12b.

Using the data shown in Fig. 12a, the following fits of  $R_{A,loss}$  as function of the amount of product water,  $m_w$ , at cold start temperatures of  $-10$ ,  $-20$ ,  $-30^\circ\text{C}$  are obtained. The fitted curves are also displayed in Fig. 12a.

$$R_{A,loss} = -0.0473 + 0.6133m_w - 0.1644m_w^2 \quad (\text{for } T_{start} = -10^\circ\text{C}) \quad [4]$$

$$R_{A,loss} = -0.0783 + 0.9768m_w - 0.4309m_w^2 \quad (\text{for } T_{start} = -20^\circ\text{C}) \quad [5]$$

$$R_{A,loss} = -0.1288 + 1.8476m_w - 1.2909m_w^2 \quad (\text{for } T_{start} = -30^\circ\text{C}) \quad [6]$$

Extrapolating the Pt area loss curves to the horizontal axis, we find that when the product water is less than 0.07 mg/cm<sup>2</sup>, there will be no ECA loss. The reason may be that when the amount of product water is very low, the ice sheets are too small in size to block proton access and hence induce no loss in ECA. In other words, protons may migrate over Pt/carbon surfaces for a very short distance without needing ionomers. This phenomenon is similar to what happens in ultrathin electrodes without ionomers. The threshold of 0.07 mg/cm<sup>2</sup> product ice as found here would be equivalent to approximately 1.9  $\mu\text{m}$  thick electrode as the theoretical ice storage in pore volumes of the 10  $\mu\text{m}$  thick cathode CL is 0.36 mg/cm<sup>2</sup>.<sup>16</sup>

A closer examination of Fig. 12b further reveals that at all startup temperatures considered in this work, there exists a sharp increase of the Pt area loss at certain product water levels, namely 0.7 mg/cm<sup>2</sup> at  $-10^\circ\text{C}$ , 0.3 mg/cm<sup>2</sup> at  $-20^\circ\text{C}$ , and 0.1 mg/cm<sup>2</sup> at  $-30^\circ\text{C}$ . It

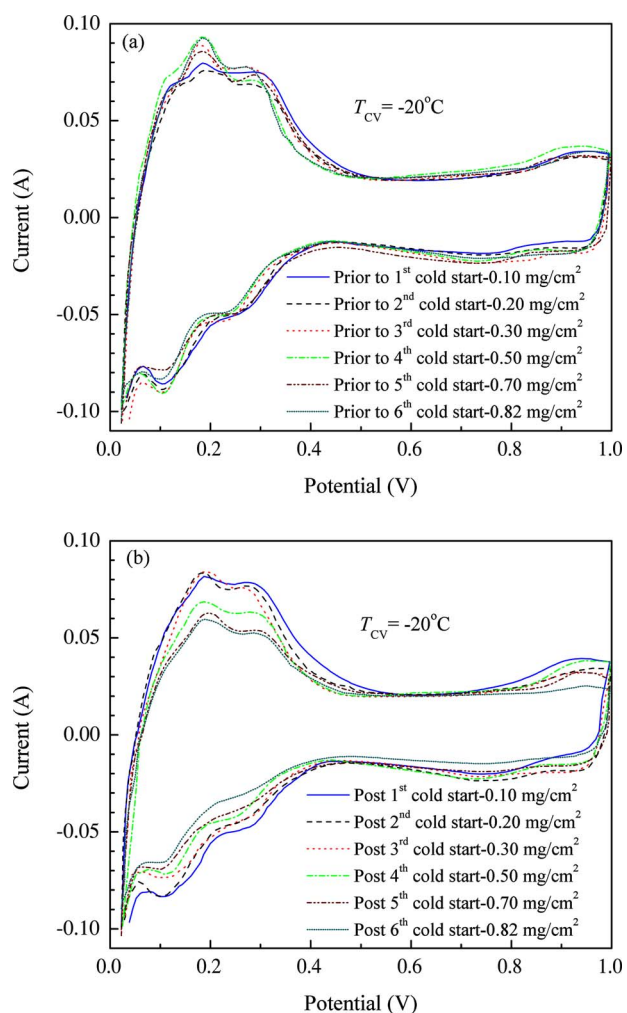


**Figure 8.** (Color online) CVs of the cathode at  $-20^{\circ}\text{C}$ : (a) prior to cold start, and (b) post-cold start. (Cold start conditions:  $T_{\text{cell}} = -20^{\circ}\text{C}$ ,  $i = 0.05 \text{ A/cm}^2$ . CV conditions:  $T_{\text{CV}} = -20^{\circ}\text{C}$ ,  $v = 50 \text{ mV/s}$ ,  $F_{\text{N}_2} = F_{\text{H}_2} = 40 \text{ mL/min}$ ,  $\text{RH}_{\text{N}_2} = \text{RH}_{\text{H}_2} = 0\%$ .)

would be interesting to determine key parameters that affect the power capability of the cathode CL post-cold start after product ice melts.

The maximum amount of product water achieved from the cold start at  $-30^{\circ}\text{C}$  is only  $0.34 \text{ mg/cm}^2$ . The cell potential during the cold start always decreases with time, as shown in Fig. 7. The voltage drop down is due not only to the Pt area loss by ice sheet formation between Pt and ionomer but more importantly to the ice formation in open pores of the cathode. For a fuel cell stack, startup without external heat depends on amount of waste heat produced before shutdown which is directly proportional to the amount of product water.<sup>20,21</sup> The amount of product water during cold start at  $-30^{\circ}\text{C}$  is much lower than at  $-20$  or  $-10^{\circ}\text{C}$ , but the temperature rise needed to break through the freezing point is much higher than  $-20$  and  $-10^{\circ}\text{C}$ . It is thus expected that successful self-startup for a fuel cell stack from  $-30^{\circ}\text{C}$  would be a challenge and requires a basic understanding of ice formation and distribution in the cathode CL. An interestingly strong correlation between isothermal single-cell experiments and nonisothermal stack operation was fully elaborated by Jiang et al.<sup>22</sup>

Returning to Fig. 12a, with the same amount of product water, cold start from  $-30^{\circ}\text{C}$  results in the highest loss of active Pt area, and from  $-10^{\circ}\text{C}$  the lowest. This implies that the amount of ice formed in the cathode CL at  $-30^{\circ}\text{C}$  is more than that at  $-10^{\circ}\text{C}$ ,

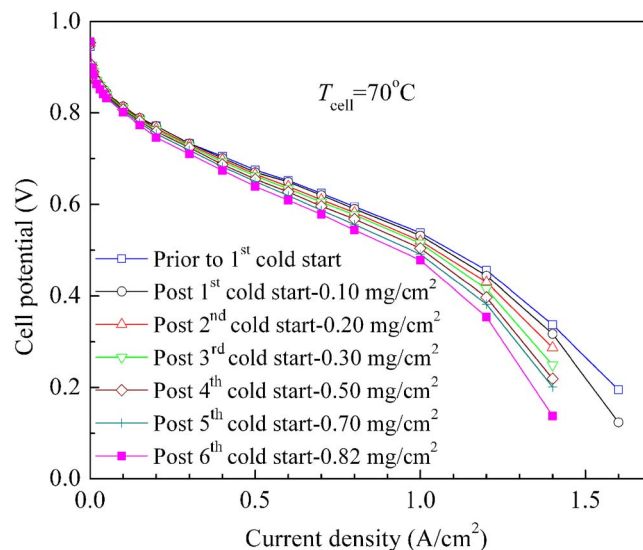


**Figure 9.** (Color online) Comparison of cell polarization curves in the cold start cycle from  $-20^{\circ}\text{C}$ . ( $T_{\text{cell}} = 70^{\circ}\text{C}$ ,  $F_{\text{H}_2} = 100 \text{ mL/min}$ ,  $F_{\text{air}} = 400 \text{ mL/min}$ ,  $\text{RH}_{\text{H}_2} = \text{RH}_{\text{air}} = 100\%$ ,  $p_{\text{H}_2} = p_{\text{air}} = 1 \text{ atm}$ ; startup temperature:  $-20^{\circ}\text{C}$ .)

despite equal product water. The reason is obvious: the amount of water absorbed by ionomer and membrane is much lower at  $-30^{\circ}\text{C}$  than that at  $-10^{\circ}\text{C}$ . Therefore, it appears that the Pt area loss measured by CV is a better indicator of the ice mass within the cathode CL than the product water. Since the ice mass in CL is believed to be the most important parameter affecting cold start performance and durability, it is expected that the CV technique developed in this work will be a useful diagnostic tool in PEFC cold start research and development.

While the active Pt area loss due to liquid water trapped between Pt particles and ionomers in the cathode can be recovered by a baking process at  $70^{\circ}\text{C}$  for 2 h, there exists permanent degradation of the electrode, resulting in consecutive Pt area loss after each cold start. The average permanent loss in the ECA per cold start operation is calculated to be 0.75%, 2.09% and 2.87% for the cold start from  $-10$ ,  $-20$ , and  $-30^{\circ}\text{C}$ , respectively. Note that the amount of product water during cold start from  $-30^{\circ}\text{C}$  is lowest, while the permanent CL degradation is highest. This strongly suggests that the CL degradation does not correlate with the product water but with the ice mass accumulated in the cathode CL. Once again, the CV technique developed from this work appears to detect product ice within the CL more directly.

One may also assess the cold-start durability from the performance data evaluated under nominal conditions. The present results show that at a cell potential of 0.5 V, the current density of the cell operated with  $\text{H}_2$  and air at  $70^{\circ}\text{C}$  before undergoing cold start is  $1.099 \text{ A/cm}^2$  (see Fig. 6). After undergoing six cold start cycles from  $-10^{\circ}\text{C}$ , the current density at  $70^{\circ}\text{C}$  decreases to  $1.02 \text{ A/cm}^2$ . There is then an average performance degradation of 1.20% per cold start under the  $-10^{\circ}\text{C}$  cold start conditions. Using the same calculation method, percentages of performance degradation under  $-20^{\circ}\text{C}$  and  $-30^{\circ}\text{C}$  cold start conditions are 2.44% and 3.70% per cold start, respectively. The tendency of increasing CL degradation due to cold start from lower temperatures, based on the  $I$ - $V$  performance evaluation, is consistent with that of Pt area measurements.

Figure 13 shows the CVs at different temperatures in a cooling-down process without cold start. It is clearly shown that H-desorption peak shifts to the right (high potential) with decreasing temperature, due partly to the increase in membrane resistance and partly to decrease in H-desorption rate. For the same reason of increased membrane resistance, the H-adsorption peak shifts toward

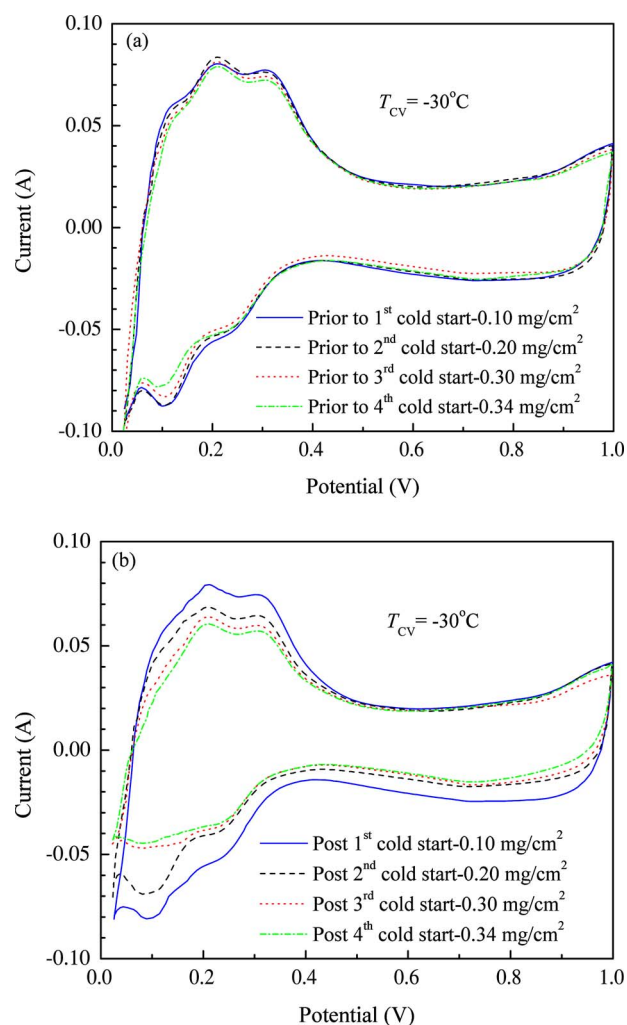


**Figure 10.** (Color online) CVs of the cathode at  $-30^{\circ}\text{C}$ : (a) prior to cold start, and (b) post-cold start. (Cold start conditions:  $T_{\text{cell}} = -30^{\circ}\text{C}$ ,  $i = 0.05 \text{ A/cm}^2$ . CV conditions:  $T_{\text{CV}} = -30^{\circ}\text{C}$ ,  $\nu = 50 \text{ mV/s}$ ,  $F_{\text{N}_2} = F_{\text{H}_2} = 40 \text{ mL/min}$ ,  $\text{RH}_{\text{N}_2} = \text{RH}_{\text{H}_2} = 0\%$ .)

lower potential. In addition, the oxidation peak due to oxidation of Pt is seen to also shift to the higher potential region with decreasing temperature, while the reduction peak for the reduction of Pt–O shifts to the low potential region with decreasing temperature. The reduction peaks occur at 0.77, 0.75, 0.74, 0.72 V at temperatures of 25,  $-10$ ,  $-20$  and  $-30^{\circ}\text{C}$ , respectively. The fact that the reduction peak shifts to the low potential at low temperature implies a decrease in oxygen reduction reaction kinetics with decreasing temperature.

Our hypothesis that ice generated in the CL during cold start contributes to the Pt area loss was further confirmed by the CV test on the anode side. Figure 14 shows the CVs for the anode prior to cold start and post sixth cold start. The cold start temperature is  $-20^{\circ}\text{C}$ . Between the first and the sixth cold start experiments, the amount of product water is 0.10, 0.20, 0.30, 0.50, 0.70 and 0.82  $\text{mg/cm}^2$ , as shown in Fig. 8 and 9. The cell temperature for CV test was  $25^{\circ}\text{C}$ . Water-saturated nitrogen and hydrogen was fed to the anode (working electrode) and cathode side (counter and reference electrodes), respectively. It is shown in Fig. 14 that no active Pt area loss of the anode was observed. We believe that this is because no ice is produced electrochemically in the anode CL during cold start, despite the fact that there is water freezing and thawing. Such experimental evidence clearly supports the view that there should be no MEA degradation resulting from freeze/thaw thermal cycling, so

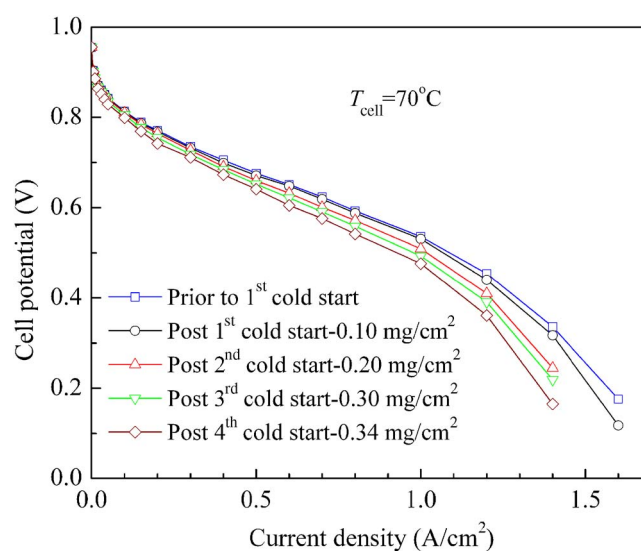


**Figure 11.** (Color online) Comparison of cell polarization curves in the cold start cycle from  $-30^{\circ}\text{C}$ . ( $T_{\text{cell}} = 70^{\circ}\text{C}$ ,  $F_{\text{H}_2} = 100 \text{ mL/min}$ ,  $F_{\text{air}} = 400 \text{ mL/min}$ ,  $\text{RH}_{\text{H}_2} = \text{RH}_{\text{air}} = 100\%$ ,  $p_{\text{H}_2} = p_{\text{air}} = 1 \text{ atm}$ ; startup temperature:  $-30^{\circ}\text{C}$ .)

long as the MEA is properly de-wetted before being subject to a subzero environment and the MEA is not fully saturated with water, a condition commonly existing in automotive PEFC stacks.

## Conclusion

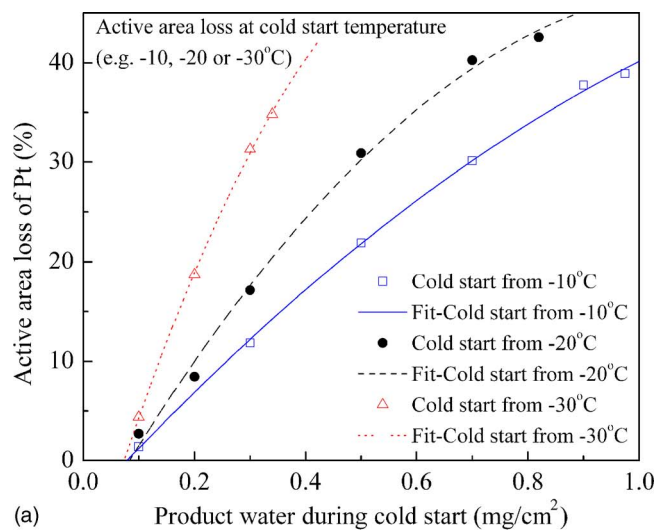
We have presented cyclic voltammetry (CV) measurements for the cathode CL during cold start and ice formation. The active Pt area measured by CV is found to decrease after cold start. This loss in Pt area is believed to be caused by the formation of ice sheets between Pt particles and ionomers in the cathode CL. Experimentally the Pt area loss is found to depend strongly on the startup temperature and product water generated during cold start. When a cell is warmed up to  $25^{\circ}\text{C}$  after cold start, the Pt area loss persists, but to a much smaller extent than immediately after cold start. Also, the Pt area loss at  $25^{\circ}\text{C}$  increases with product water generated during cold start. This is believed to be caused by the presence of liquid water trapped between Pt particles and ionomers as a result of ice melting. We found no active Pt area loss in the anode CL, which again can be explained by the fact that no ice is produced electrochemically in the anode.

Both types of Pt area loss can be largely recovered by operating the cell at  $70^{\circ}\text{C}$  and high current density for an extended period of time (baking), indicating that liquid water trapped between Pt particles and ionomers can be removed under elevated temperature and reaction heat. However, permanent CL degradation, at levels ranging from 1 to 3% per cold start, is also observed. The degree of permanent degradation strongly correlates with the ice volume inside the CL created during cold start.

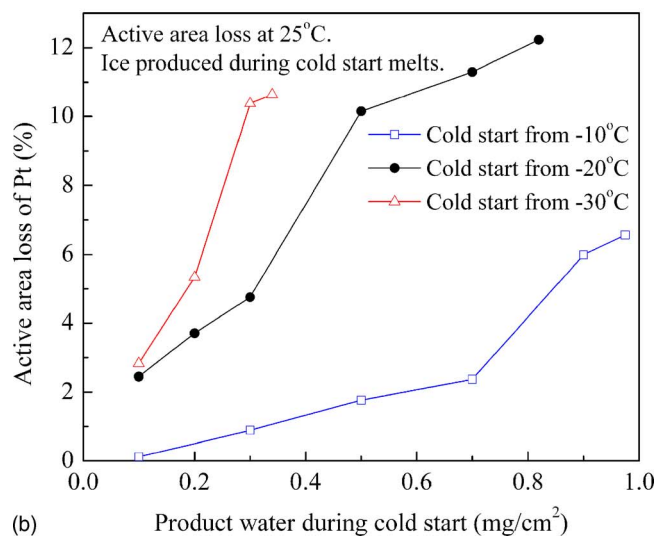
The electrochemically active Pt area calculated from CV remains roughly the same between  $25^{\circ}\text{C}$  and  $-30^{\circ}\text{C}$  prior to cold start, and thus is temperature independent, as expected.

## Acknowledgments

Financial support of this work by Nissan Motor Co. Ltd. is gratefully acknowledged. The authors also acknowledge fruitful discussions with Y. Tabuchi.



(a)



(b)

**Figure 12.** (Color online) Pt active area loss at (a) startup temperature after cold start, and (b) 25°C.

The Pennsylvania State University assisted in meeting the publication costs of this article.

### References

- M. Oszcipok, D. Riemann, U. Kronenwett, M. Kreideweis, and M. Zedda, *J. Power Sources*, **145**, 407 (2005).
- M. Oszcipok, M. Zedda, D. Riemann, and D. Geckeler, *J. Power Sources*, **154**, 404 (2006).
- F. Kagami, Y. Hishinuma, and T. Chikahisa, *Therm. Sci. Eng.*, **10**, 25 (2002).
- Y. Hishinuma, T. Chikahisa, F. Kagami, and T. Ogawa, *JSME Int. J., Ser. B*, **47**, 235 (2004).
- R. C. McDonald, C. K. Mittelsteadt, and E. L. Thompson, *Fuel Cells*, **4**, 208 (2004).
- M. S. Wilson, J. A. Valerio, and S. Gottesfeld, *Electrochim. Acta*, **40**, 355 (1995).
- E. A. Cho, J. J. Ko, H. Y. Ha, S. A. Hong, K. Y. Lee, T. W. Lim, and I. H. Oh, *J. Electrochem. Soc.*, **150**, A1667 (2003).
- E. A. Cho, J. J. Ko, H. Y. Ha, S. A. Hong, K. Y. Lee, T. W. Lim, and I. H. Oh, *J. Electrochem. Soc.*, **151**, A661 (2004).
- Q. Guo and Z. Qi, *J. Power Sources*, **160**, 1269 (2006).
- J. St-Pierre, J. Roberts, K. Colbow, S. Campbell, and A. Nelson, *J. New Mater. Electrochem. Syst.*, **8**, 163 (2005).
- L. Mao, K. Tajiri, S. H. Ge, X. G. Yang, and C. Y. Wang, Abstract 998, The Electrochemical Society Meeting Abstracts, Vol. 2005-2 Los Angeles, Oct 16–21, 2005.
- M. Cappadonia, J. W. Erning, S. M. S. Niaki, and U. Stimming, *Solid State Ionics*, **77**, 65 (1995).
- M. Cappadonia, J. W. Erning, and U. Stimming, *J. Electroanal. Chem.*, **376**, 189 (1994).
- M. Saito, K. Hayamizu, and T. Okada, *J. Phys. Chem. B*, **109**, 3112 (2005).
- E. L. Thompson, T. W. Capehart, T. J. Fuller, and J. Jorne, *J. Electrochem. Soc.*, **153**, A2351 (2006).
- S. H. Ge and C. Y. Wang, *Electrochem. Solid-State Lett.*, **9**, A499 (2006).
- S. H. Ge and C. Y. Wang, *Electrochim. Acta*, **52**, 4825 (2007).
- L. Mao and C. Y. Wang, *J. Electrochem. Soc.*, **154**, B139 (2007).
- L. Mao, C. Y. Wang, and Y. Tabuchi, *J. Electrochem. Soc.*, **154**, B341 (2007).
- K. Tajiri, Y. Tabuchi, and C. Y. Wang, *J. Electrochem. Soc.*, **154**, B147 (2007).
- K. Tajiri, Y. Tabuchi, F. Kagami, S. Takahashi, K. Yoshizawa, and C. Y. Wang, *J. Power Sources*, **165**, 279 (2007).
- F. M. Jiang, W. F. Fang, and C. Y. Wang, *Electrochim. Acta*, In press.

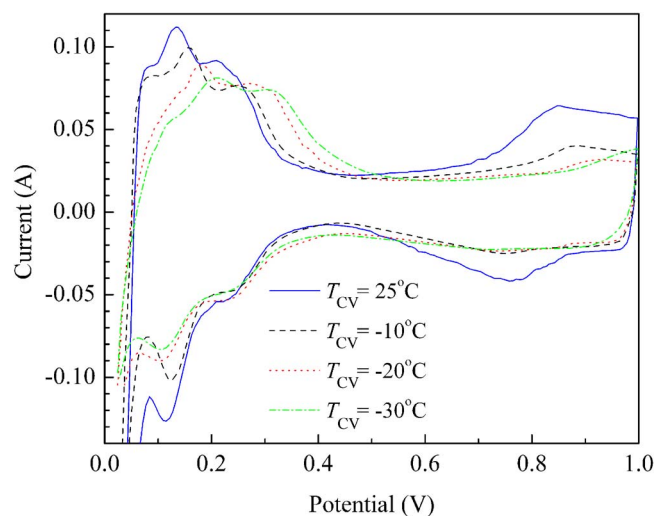


**Figure 13.** (Color online) Comparison of CV diagrams at different temperatures without cold start. (CV conditions:  $\nu = 50$  mV/s.)

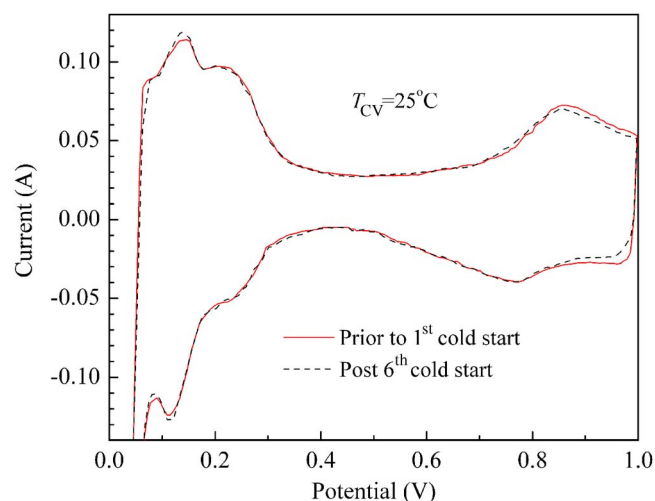


**Figure 14.** (Color online) Comparison of CVs of the anode at 25°C prior to first cold start and post sixth cold start. Between the first and the sixth cold start, the amount of produced water is 0.10, 0.20, 0.30, 0.50, 0.70 and 0.82  $\text{mg}/\text{cm}^2$ , respectively. The startup temperature is -20°C. (CV conditions:  $T_{CV} = 25^\circ\text{C}$ ,  $\nu = 50$  mV/s,  $F_{N_2} = F_{H_2} = 100$  mL/min,  $RH_{N_2} = RH_{H_2} = 100\%$ .)